PRAMANA — journal of physics

Vol. 77, No. 2
August 2011
pp. 297–313

Rapidity dependence of multiplicity fluctuations and correlations in high-energy nucleus–nucleus interactions

DIPAK GHOSH[1], ARGHA DEB[1], SWARNAPRATIM BHATTACHARYYA[2,*] and UTPAL DATTA[1]

[1]Department of Physics, Nuclear and Particle Physics Research Centre, Jadavpur University, Kolkata 700 032, India
[2]Department of Physics, New Alipore College, L Block, New Alipore, Kolkata 700 053, India
*Corresponding author. E-mail: swarna_pratim@yahoo.com

MS received 28 April 2010; revised 10 February 2011; accepted 23 February 2011

Abstract. The multiplicity fluctuations of the produced pions were studied using scaled variance method in ^{16}O–AgBr interactions at 2.1 AGeV, ^{24}Mg–AgBr interactions at 4.5 AGeV, ^{12}C–AgBr interactions at 4.5 AGeV, ^{16}O–AgBr interactions at 60 AGeV and ^{32}S–AgBr interactions at 200 AGeV at two different binning conditions. In the first binning condition, the rapidity interval was varied in steps of one centring about the central rapidity until it reached 14. In the second case, the rapidity interval was increased in steps of 1.6 up to 14.4. Multiplicity distributions and their scaled variances were presented as a function of the dependence on the rapidity width for both the binning conditions. Multiplicity fluctuations were found to increase with the increase of rapidity interval and later found to saturate at larger rapidity window for all the interactions and in both the binning conditions. Multiplicity fluctuations were found to increase with the energy of the projectile beam. The values of the scaled variances were found to be greater than one in all the cases in both the binning conditions indicating the presence of correlation during the multiparticle production process in high-energy nucleus–nucleus interactions. Experimental results were compared with the results obtained from the Monte Carlo simulated events for all the interactions. The Monte Carlo simulated data showed very small values of scaled variance suggesting very small fluctuations for the simulated events. Experimental results obtained from ^{16}O–AgBr interactions at 60 AGeV and ^{32}S–AgBr interactions at 200 AGeV were compared with the events generated by Lund Monte Carlo code (FRITIOF model). FRITIOF model failed to explain the multiplicity fluctuations of pions emitted from ^{16}O–AgBr interactions at 60 AGeV for both the binning conditions. However, the experimental data agreed well with the FRITIOF model for ^{32}S–AgBr interactions at 200 AGeV.

Keywords. Fluctuations; scaled variance; multiplicity.

PACS Nos 25.75.-q; 25.75.Ag; 25.75.Gz; 24.60.Ky

1. Introduction

The multiplicity of charged particles in high-energy nucleus–nucleus interactions is an important variable which indicates how many particles are produced in that interaction.

DOI: 10.1007/s12043-011-0131-2; *e*Publication: 2 August 2011

The multiplicity distribution is said to be the basic measurable quantity in high-energy interactions. It plays a fundamental role in extracting the first information on the underlying particle production mechanism. The study of multiplicity fluctuations has become an important tool to know the internal dynamics of multiparticle production process. The goal of the current heavy-ion collision physics is to study the properties of the phase transition between the quark–gluon plasma (QGP) phase and the ordinary hadronic phase. In many-body systems, phase transition often causes more dramatic changes in the fluctuations of an observable than in the average of an observable. For instance, as a system goes through a phase transition, heat capacity changes abruptly whereas the energy density remains a smooth function of the temperature. Therefore, fluctuation measurements in heavy-ion collisions have a good chance of being the signals of the QGP formation. Interesting fluctuation variables considered so far include multiplicity fluctuations, energy fluctuations, charge fluctuations and mean transverse momentum fluctuations. In idealized situations, these fluctuations can reveal the following properties of the underlying system: if a thermal equilibrium is reached, the multiplicity distribution is very close to a Poisson distribution. Therefore, the multiplicity fluctuation can tell us whether a global thermalization has been achieved [1]. Energy fluctuation is related to the specific heat. Lattice QCD calculations show that the specific heat has a sharp peak around the critical temperature. The energy fluctuations therefore have the potential of being a clear signal of the phase transition. Non-statistical mean transverse momentum fluctuations can signal the existence of the tricritical point. Charge fluctuations are sensitive to the unit charge of the underlying system. Quarks have fractional electric and baryonic charges. Therefore, the fluctuations of those charges in a QGP and a hadronic matter are clearly distinguishable. All these are interesting and deserve careful study.

There has been evidence for the occurrence of multiplicity fluctuations in the pseudorapidity distributions. The existence of such fluctuations would give information on the substructure in space time of collision region. Large fluctuations in pseudorapidity window have been observed in cosmic ray events and in hadron–hadron, nucleus–nucleus and hadron–nucleus interactions at accelerator energies. They have been interpreted in terms of several models: as a possible indication of hadronic phase transition, as Cherenkov radiation or simply originating from a cascade mechanism. The rapid development in the field of pion multiplicity fluctuations in recent years is related to the large amount of high multiplicity data from the well-known heavy-ion experiments at CERN-SPS and BNL-RHIC. Although some progress has been made in understanding the fluctuation phenomena, still a lot of questions remain unanswered.

In statistical models, the width of the multiplicity distribution depends on the conservation laws that the system obeys. It has been observed that multiplicity fluctuations are largest in grand canonical ensemble and smallest in canonical ensemble [2]. These theoretical considerations motivated vigorous studies of multiplicity fluctuations from experimental and theoretical points of view [3–7]. Much theoretical interest has been directed towards the fluctuation study motivated by the near perfect Gaussian distribution of transverse momentum and particle ratio [8,9] measured at SPS. For these Gaussian distributions, the variances or the width of the distributions contain information about the reaction mechanism as well as the nuclear geometry [10–12].

A useful measure of fluctuation of any variable is the ratio of its variance to its mean [2]. So the variance of the multiplicity distribution can be used to measure the multiplicity

fluctuations. To study the multiplicity fluctuations in high-energy collisions, we define a scaled variable ω such that

$$\omega = \frac{\langle n^2 \rangle - \langle n \rangle^2}{\langle n \rangle}, \tag{1}$$

where $\langle n \rangle$ is the average multiplicity. A direct measure of the scaled variable would give a direct measure of multiplicity fluctuations. Multiplicity fluctuation can be interpreted as an aspect of a two-particle correlation function. The strength of multiplicity fluctuations comes from the physical insight that gives to the changes in the two-particle correlations. In other words, physical interpretation of the changes in the two-particle correlations is often most apparent in terms of the multiplicity fluctuations. Now, to find how the study of multiplicity fluctuations can reflect the existence of two-particle correlation, we have to consider the multiplicity distribution of the produced pions. It is known that if the particles are produced independently, the multiplicity distribution is Poissonian. On the contrary, if the production of one particle enhances the probability to produce other particles then the distribution is broader than Poissonian. In many models the scaled variances are independent of the number of particle production sources and the multiplicity distribution can be described by a Poissonian distribution. The variance of a Poissonian distribution is equal to its mean and consequently $\omega = 1$. If ω is greater than 1, the multiplicity distribution is broader than Poissonian and if ω is less than 1, the multiplicity distribution is narrower than the Poissonian. The study of scaled variance can very easily indicate the nature of correlation among the produced particles. If the value of ω is far greater than 1, it may be said that there is pronounced correlation among the produced particles. On the contrary, if the value of ω is close to 1, feeble correlation is indicated.

The multiplicity fluctuation has been studied in terms of the scaled variances for most central Pb+Pb collisions at 20 AGeV, 30 AGeV, 40 AGeV, 80 AGeV and 158 AGeV by the NA49 experiment at CERN SPS [2]. The scaled variance of multiplicity distribution was found to increase with decreasing rapidity and transverse momenta. The outcome of the analysis [2] has attracted much attention in recent times. It will be interesting to study the rapidity dependence effect of scaled variance at a wide range of energy. In this paper we have studied the rapidity dependence of multiplicity fluctuation of the produced pions from ^{16}O–AgBr interactions at 2.1 AGeV, ^{24}Mg–AgBr interactions at 4.5 AGeV, ^{12}C–AgBr interactions at 4.5 AGeV, ^{16}O–AgBr interactions at 60 AGeV and ^{32}S–AgBr interactions at 200 AGeV using scaled variance method at two different binning conditions. In the first binning condition, the rapidity interval was increased in steps of 1 centring about the central rapidity. In the second case, the rapidity interval was increased in steps of 1.6. We have also tried to study the presence of correlation among the produced pions at that energy regime. Later, experimental results were compared with the results obtained from the Monte Carlo simulated events for all the interactions and also for both the binning conditions. Experimental results obtained from ^{16}O–AgBr interactions at 60 AGeV and ^{32}S–AgBr interactions at 200 AGeV were also compared with the events generated by Lund Monte Carlo code (FRITIOF model).

2. Experimental details

Illford G5 nuclear photographic emulsion plates were irradiated horizontally with a beam of ^{16}O nuclei at 2.1 AGeV energy obtained from Bevalac Berkley [13]. The data for

^{24}Mg–AgBr interactions [14] and ^{12}C–AgBr interactions [15] were obtained by exposing NIKFIBR2 plates at 4.5 AGeV obtained from JINR Dubna, Russia. The data of ^{16}O–AgBr interactions at 60 AGeV and ^{32}S–AgBr interactions at 200 AGeV were obtained by exposing 60 AGeV oxygen beam and 200 AGeV sulphur beam on Ilford G5 emulsion stacks at CERN SPS [16].

A Leitz Ortholux microscope with a 10× objective and 25× ocular lens provided with a Brower travelling stage was used to scan the plates of ^{16}O–AgBr interactions at 2.1 AGeV. A Leitz Metalloplan microscope with a 10× objective and 10× ocular lens provided with a semi-automatic scanning stage was used to scan the other four interaction plates. Each plate was scanned by two independent observers to increase the scanning efficiency. The final measurements were done using an oil-immersion 100× objective. The measuring system fitted with it has 1 μm resolution along the X and Y-axes and 0.5 μm resolution along the Z-axis.

Events were chosen according to the following criteria:

(a) The incident beam track should not exceed more than 3° from the main beam direction in the pellicle. This criterion ensured that we selected the real projectile beam.
(b) Events showing interactions within 20 μm from the top and bottom surfaces of the pellicle were rejected to reduce the loss of tracks as well as to reduce the errors in the measurement of emission and azimuthal angles.
(c) The tracks of the incident particle, which induce interactions, were followed in the backward direction to ensure that it was a projectile beam starting from the beginning of the pellicle.

According to the emulsion terminology [17], the particles emitted after interactions are classified as:

Shower particles. The tracks of particles having ionization $I \leq 1.4I_0$ are called shower tracks. I_0 is the minimum ionization of a singly charged particle. They are mostly due to pions with a small admixture of K-mesons and fast protons. These shower particles are produced in a forward cone. The velocities of these particles are greater than $0.7c$ where c is the velocity of light in free space. Because of high velocity, these particles are not generally confined within the emulsion pellicle. These particles have minimum ionization and hence they are the most energetic. Their energy is in GeV range.

Black particles. Black particles consist of both singly and multiply charged fragments. They are fragments of various elements like carbon, lithium, beryllium etc. with ionization $\geq 10I_0$. These black particles have the maximum ionizing power. So they are less energetic and consequently they are short-ranged. Ranges of black particles are less than 3 mm in the emulsion medium. The velocities of the black particles are less than $0.3c$. In the emulsion experiments it is very difficult to measure the charge of the fragments. So identification of the exact nucleus is not possible.

Grey particles. They are mainly fast target recoil protons with energy upto 400 MeV. They have ionization $1.4I_0 \leq I < 10I_0$. Their ranges are greater than 3 mm and their velocities are between $0.3c$ and $0.7c$.

Projectile fragments. Along with these tracks there are a few projectile fragments. In high-energy nuclear collisions the projectile beam which collides with the target nucleus also undergoes fragmentation. These particles have constant ionization, long range and small emission angle. They generally lie within 3° with respect to the main beam direction. Great care should be taken to identify these projectile fragments.

Event-by-event analysis demands the separation of events into ensembles of collisions of different projectiles with hydrogen (H), light nuclei (CNO) and heavy nuclei (AgBr). Usually events with $N_h \leq 1$ are classified as collision with hydrogen. Events with $2 \leq N_h \leq 7$ are classified as collisions with light nuclei and $N_h \geq 8$ as collisions with heavy nuclei, where N_h is the total number of heavy tracks, i.e. total number of black and grey tracks. In this method the separation of events for AgBr target is quite accurate in the sample with $N_h > 8$ but when $N_h \leq 8$ there is an admixture of CNO events and peripheral collisions with AgBr target. In this experiment only events with $N_h > 8$, have been selected to exclude CNO interactions and peripheral collisions with AgBr target. The percentage of occurrence of events with $N_h \leq 1$ is (0–5)% in the total data sample. The percentage of occurrence of CNO and AgBr events are (15–25)% and (70–85)%, respectively in the total data sample of the projectile–emulsion interactions. The probability of events due to collision with AgBr targets increases slowly with the increase of projectile mass at similar energy. In this analysis we have focussed our attention to the events generating from the collisions with the AgBr nuclei only and have discarded all other types of events. So, according to the selection procedure mentioned above we have chosen 730 events of ^{16}O–AgBr interactions at 2.1 AGeV [13], 800 events of ^{24}Mg–AgBr interactions at 4.5 AGeV [18], 800 events of ^{12}C–AgBr interactions at 4.5 AGeV [19], 250 events of ^{16}O–AgBr interactions at 60 AGeV [20] and 140 events of ^{32}S–AgBr interactions at 200 AGeV [21]. The emission angle (θ) and azimuthal angle (ϕ) are measured for each track with respect to the beam directions by taking readings of the coordinates of the interaction point (X_0, Y_0, Z_0), coordinates (X_1, Y_1, Z_1) at the end of the linear portion of each secondary track and coordinate (X_i, Y_i, Z_i) of a point on the incident beam. In pion multiplicity distribution the phase space variable used is the pseudorapidity η. It is related with the emission angle θ (measured with respect to the beam direction) by the relation $\eta = -\ln\tan(\theta/2)$. Nuclear emulsion experiments, in spite of a few limitations, are superior to many experiments in one respect that they offer a very high angular resolution (around 1 mrad), and this advantage can be exploited where the distribution of particles in small phase space region has to be considered. Also as a detector it is capable of registering all the produced or emitted particles in the 4π geometry.

3. Results and discussion

To study the multiplicity fluctuations of the produced pions from ^{16}O–AgBr interactions at 2.1 AGeV, ^{24}Mg–AgBr interactions at 4.5 AGeV, ^{12}C–AgBr interactions at 4.5 AGeV, ^{16}O–AgBr interactions at 60 AGeV and ^{32}S–AgBr interactions at 200 AGeV in various rapidity window sizes, several overlapping pseudorapidity interval centring about the central rapidity values were taken. The central rapidity value can be easily obtained from the pseudorapidity distribution of the concerned data set. The pseudorapidity distribution

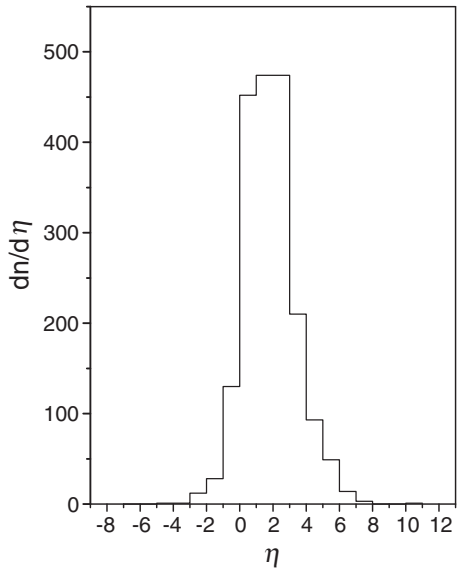

Figure 1. The rapidity distribution for ^{16}O–AgBr interactions at 2.1 AGeV.

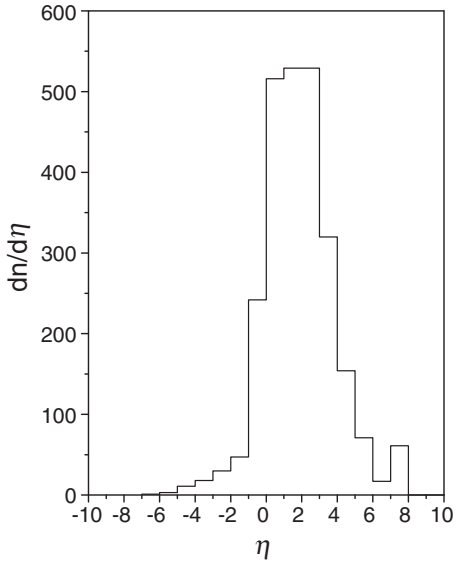

Figure 2. The rapidity distribution for ^{24}Mg–AgBr interactions at 4.5 AGeV.

of ^{16}O–AgBr interactions at 2.1 AGeV, ^{24}Mg–AgBr interactions at 4.5 AGeV, ^{12}C–AgBr interactions at 4.5 AGeV, ^{16}O–AgBr interactions at 60 AGeV and ^{32}S–AgBr interactions at 200 AGeV are shown in figures 1–5 respectively. To determine the central rapidity value,

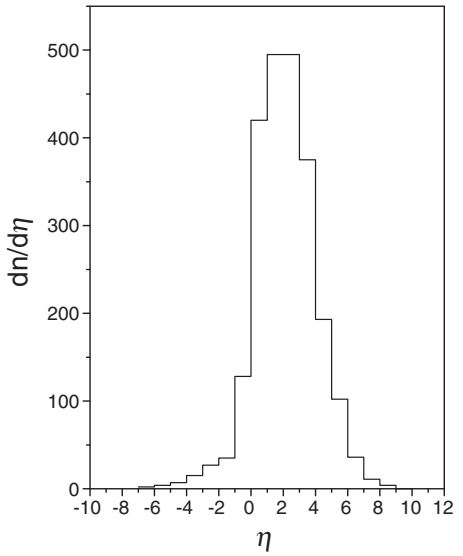

Figure 3. The rapidity distribution for ^{12}C–AgBr interactions at 4.5 AGeV.

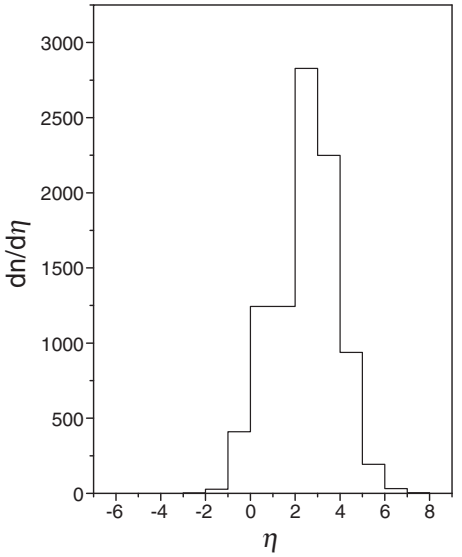

Figure 4. The rapidity distribution for ^{16}O–AgBr interactions at 60 AGeV.

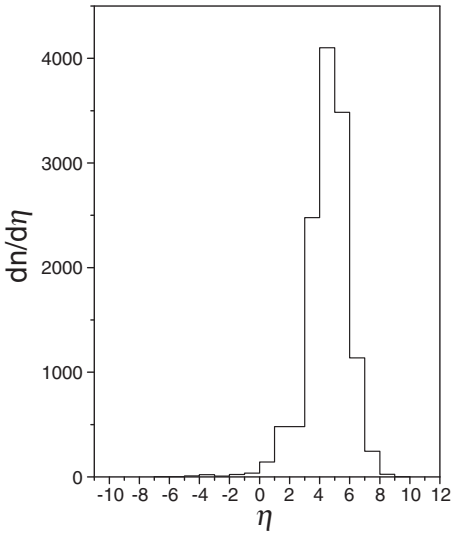

Figure 5. The rapidity distribution for ^{32}S–AgBr interactions at 200 AGeV.

the total rapidity range was divided into small non-overlapping intervals. Number of particles in each interval was calculated. The central rapidity value is that value where the number of particles are maximum. The central rapidity value for ^{16}O–AgBr interactions at 2.1 AGeV, ^{24}Mg–AgBr interactions at 4.5 AGeV, ^{12}C–AgBr interactions at 4.5 AGeV, ^{16}O–AgBr interactions at 60 AGeV and ^{32}S–AgBr interactions at 200 AGeV are 1.17, 2.2, 1.57, 1.98 and 4.71 respectively. Size of a rapidity interval, sometimes called as rapidity window, centring about the central rapidity value, is designated by $\Delta\eta$. The span of $\Delta\eta$ has been taken from the narrowest width to the widest width for each beam except for the extreme zones of projectile or target fragmentation, covering almost the full length of pseudorapidity.

We have calculated the average multiplicity $\langle n\rangle$, the variance $\langle n^2\rangle - \langle n\rangle^2$, and the scaled variance according to eq. (1) for all the interactions within a rapidity interval. The rapidity interval was constructed in the following way. The interval size was designated as $\Delta\eta = \eta_1 \leq \eta_c \leq \eta_2$ with $\eta_1 = \eta_c - 0.5$ and $\eta_2 = \eta_c + 0.5$. Here η_c is the central rapidity value. The value of $\Delta\eta$ was increased in steps of 1 till it reached 14. The scaled variance (ω) was calculated in each of this rapidity interval for all the interactions. When analysing the data, any shower track falling within the very forward cone of emission angle was excluded because in this region there may be an admixture of pions and projectile fragments. We have shown the values of scaled variance for each of the window size and for each interaction in table 1. From table 1 it can be noted that for ^{16}O–AgBr interactions at 2.1 AGeV and 60 AGeV the maximum fluctuation occurs in the rapidity interval $-0.3 \leq \eta_c \leq 2.7$ (i.e. $\Delta\eta = 3$) and $1 \leq \eta_c \leq 3$ ($\Delta\eta = 2$) respectively. In ^{12}C–AgBr interactions, the maximum fluctuations have been noted in the rapidity space $0.6 \leq \eta_c \leq 2.6$ (i.e. $\Delta\eta = 2$). However, for ^{24}Mg–AgBr interactions, the maximum fluctuations occur at $-0.8 \leq \eta_c \leq 5.2$ ($\Delta\eta = 6$). In ^{32}S–AgBr interactions at 200 AGeV, the maximum fluctuations occur at the rapidity range $1.7 \leq \eta_c \leq 7.7$ ($\Delta\eta = 6$). It is also seen from table 1 that at low energy the multiplicity fluctuation

Table 1. The values of scaled variance in different interactions and in different window sizes when rapidity interval is varied in steps of 1 centring about the central rapidity.

Window size $\Delta\eta$	^{16}O–AgBr interactions at 2.1 AGeV	^{24}Mg–AgBr interactions at 4.5 AGeV	^{12}C–AgBr interactions at 4.5 AGeV	^{16}O–AgBr interactions at 60 AGeV	^{32}S–AgBr interactions at 200 AGeV
1	2.05 ± 0.002	1.8 ± 0.001	2.23 ± 0.004	12.25 ± 0.010	8.62 ± 0.010
2	3.16 ± 0.006	3.3 ± 0.003	3.94 ± 0.008	12.48 ± 0.012	12.8 ± 0.011
3	3.209 ± 0.008	4.34 ± 0.007	3.82 ± 0.010	10.26 ± 0.015	15.71 ± 0.015
4	3.099 ± 0.012	4.52 ± 0.009	3.46 ± 0.014	8.74 ± 0.018	18.9 ± 0.017
5	2.904 ± 0.013	4.6 ± 0.013	3.48 ± 0.019	7.92 ± 0.021	23.72 ± 0.018
6	2.73 ± 0.017	4.64 ± 0.018	3.45 ± 0.019	7.47 ± 0.025	25.23 ± 0.018
7	2.55 ± 0.019	4.56 ± 0.019	3.23 ± 0.021	7.34 ± 0.025	25.03 ± 0.022
8	2.47 ± 0.019	4.52 ± 0.023	3.22 ± 0.024	7.27 ± 0.026	24.77 ± 0.023
9	2.396 ± 0.022	4.48 ± 0.027	2.91 ± 0.026	7.27 ± 0.026	24.67 ± 0.026
10	2.37 ± 0.027	4.42 ± 0.029	2.99 ± 0.027	7.27 ± 0.027	24.6 ± 0.027
11	2.36 ± 0.028	4.39 ± 0.031	3.00 ± 0.033	7.268 ± 0.028	24.55 ± 0.029
12	2.36 ± 0.028	4.35 ± 0.033	3.03 ± 0.037	7.266 ± 0.028	24.47 ± 0.032
13	2.33 ± 0.032	4.4 ± 0.035	3.01 ± 0.039	7.266 ± 0.029	24.38 ± 0.035
14	2.33 ± 0.033	4.39 ± 0.035	3.04 ± 0.039	7.266 ± 0.031	24.35 ± 0.037

is small. Multiplicity fluctuation increases as energy of the projectile beam increases. As energy increases more and more pions are produced. As the number of pions increases, the probability of correlated emission also increases.

In table 2 we have shown the maximum values of the scaled variance ($\omega_{\max}$) and the range of $\Delta\eta$ values for all the interactions. From table 2 it is seen that the values of $\omega_{\max}$ is lowest for ^{16}O–AgBr at 2.1 AGeV. For ^{12}C–AgBr, $\omega_{\max} = 3.94$ and for ^{24}Mg–AgBr interactions, $\omega_{\max} = 4.64$. This is very interesting. Both ^{12}C–AgBr and ^{24}Mg–AgBr interactions have the same energy. The higher value of $\omega_{\max}$ in ^{24}Mg–AgBr interactions may be due to the fact that the size of the magnesium nucleus is double that of the carbon nucleus. For ^{16}O–AgBr interaction at 60 AGeV and ^{32}S–AgBr interactions at 200 AGeV, the values of $\omega_{\max}$

Table 2. The maximum value of scaled variance for different interactions and at different rapidity width where maximum fluctuations occurred when rapidity interval is varied in steps of 1 centring about the central rapidity.

Interactions	Energy (AGeV)	$\Delta\eta$ range	$\omega_{\max}$
^{16}O–AgBr	2.1	$-0.3 \leq \eta_c \leq 2.7$	3.209 ± 0.008
^{12}C–AgBr	4.5	$0.6 \leq \eta_c \leq 2.6$	3.94 ± 0.008
^{24}Mg–AgBr	4.5	$-0.8 \leq \eta_c \leq 5.2$	4.64 ± 0.018
^{16}O–AgBr	60	$1 \leq \eta_c \leq 3$	12.48 ± 0.012
^{32}S–AgBr	200	$1.7 \leq \eta_c \leq 7.7$	25.23 ± 0.018

increase significantly. Higher values of $\omega_{\max}$ indicate large fluctuations for that specified interactions. The correlated emission of pions signifies the dynamical fluctuations.

Comparisons of experimental results have been made with event samples simulated by generating random numbers for all the interactions. In all the cases, the phase space variable associated with each shower track in an event has been replaced by a random number, assuming independent emission of particles. The simulated event sample has the same size and identical shower multiplicity distribution as the experimental one. The values of the scaled variance ω have been calculated for the simulated events for ^{16}O–AgBr interactions at 2.1 AGeV, ^{24}Mg–AgBr interactions at 4.5 AGeV, ^{12}C–AgBr interactions at 4.5 AGeV, ^{16}O–AgBr interactions at 60 AGeV and ^{32}S–AgBr interactions at 200 AGeV and are tabulated in table 3. Comparing tables 1 and 3, it can be noted that the scaled variance for simulated events are much smaller than that of the experimental events for all the interactions. From tables 1 and 2 it can be seen that for ^{16}O–AgBr interactions at 60 AGeV and for ^{12}C–AgBr interactions at 4.5 AGeV, the maximum fluctuations occur at $\Delta\eta = 2$ for the experimental data sets. For ^{16}O–AgBr interactions at 2.1 AGeV pronounced fluctuations are found to occur at $\Delta\eta = 3$. However, for simulated events of ^{16}O–AgBr interactions at 60 AGeV and for ^{12}C–AgBr interactions at $\Delta\eta = 2$, the multiplicity fluctuations are very small. In ^{16}O–AgBr interactions at 2.1 AGeV the values of the scaled variance are even less than 1 at $\Delta\eta = 3$ indicating uncorrelated particle production in the simulated events. For ^{24}Mg–AgBr and ^{32}S–AgBr interactions at $\Delta\eta = 6$, the fluctuations are maximum for the experimental data sets. But for the simulated data sets at the rapidity window $\Delta\eta = 6$ the values of the scaled variance are small.

Table 3. The values of scaled variance in different interactions and in different window sizes for the simulated events when rapidity interval is varied in steps of 1 centring about the central rapidity.

Window size $\Delta\eta$	^{16}O–AgBr interactions at 2.1 AGeV (simulated events)	^{24}Mg–AgBr interactions at 4.5 AGeV (simulated events)	^{12}C–AgBr interactions at 4.5 AGeV (simulated events)	^{16}O–AgBr interactions at 60 AGeV (simulated events)	^{32}S–AgBr interactions at 200 AGeV (simulated events)
1	0.493 ± 0.002	0.323 ± 0.001	0.239 ± 0.001	1.036 ± 0.002	1.10 ± 0.003
2	0.711 ± 0.005	0.733 ± 0.003	0.612 ± 0.004	1.53 ± 0.005	1.65 ± 0.004
3	0.903 ± 0.005	1.09 ± 0.004	0.833 ± 0.005	1.99 ± 0.007	2.16 ± 0.005
4	0.942 ± 0.007	1.24 ± 0.006	1.023 ± 0.007	2.68 ± 0.008	2.81 ± 0.009
5	1.07 ± 0.008	1.37 ± 0.009	1.2 ± 0.008	3.43 ± 0.008	3.66 ± 0.010
6	1.13 ± 0.010	1.63 ± 0.010	1.325 ± 0.010	3.89 ± 0.009	3.94 ± 0.012
7	1.28 ± 0.012	1.76 ± 0.011	1.51 ± 0.011	4.25 ± 0.009	4.43 ± 0.016
8	1.42 ± 0.012	1.96 ± 0.013	1.55 ± 0.012	4.72 ± 0.010	4.98 ± 0.017
9	1.48 ± 0.014	2.12 ± 0.015	1.61 ± 0.015	5.08 ± 0.011	5.6 ± 0.019
10	1.475 ± 0.017	2.37 ± 0.017	1.81 ± 0.017	5.43 ± 0.012	5.96 ± 0.021
11	1.52 ± 0.018	2.53 ± 0.017	1.95 ± 0.018	5.93 ± 0.015	6.38 ± 0.022
12	1.64 ± 0.018	2.74 ± 0.019	1.98 ± 0.019	6.30 ± 0.017	6.65 ± 0.022
13	1.85 ± 0.017	3.05 ± 0.019	1.97 ± 0.020	6.72 ± 0.018	7.15 ± 0.024
14	1.94 ± 0.019	3.17 ± 0.019	2.04 ± 0.021	7.20 ± 0.021	7.59 ± 0.024

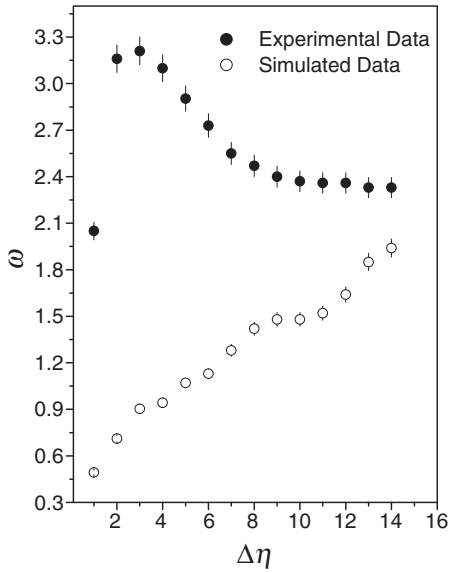

Figure 6. The variation of scaled variance with rapidity window for ^{16}O–AgBr interactions at 2.1 AGeV for the experimental and the simulated events when rapidity interval is varied in steps of 1 centring about the central rapidity.

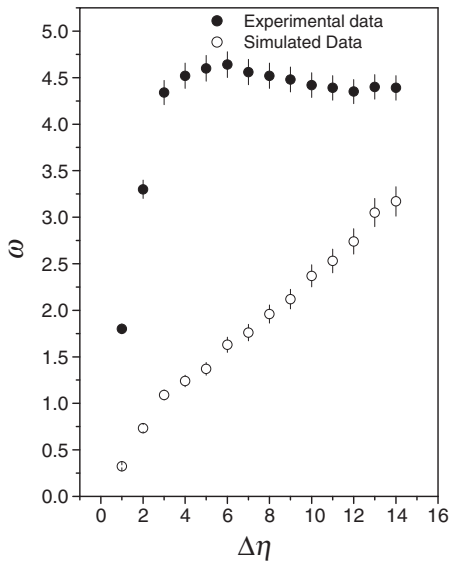

Figure 7. The variation of scaled variance with rapidity window for ^{24}Mg–AgBr interactions at 4.5 AGeV for the experimental and the simulated events when rapidity interval is varied in steps of 1 centring about the central rapidity.

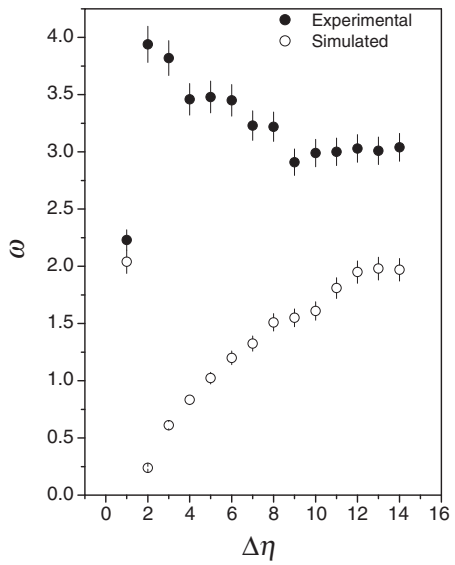

Figure 8. The variation of scaled variance with rapidity window for ^{12}C–AgBr interactions at 4.5 AGeV for the experimental and the simulated events when rapidity interval is varied in steps of 1 centring about the central rapidity.

We have plotted the experimentally obtained scaled variance ω with the rapidity window size in figure 6 for ^{16}O–AgBr interactions at 2.1 AGeV, in figure 7 for ^{24}Mg–AgBr interactions, in figure 8 for ^{12}C–AgBr interactions, in figure 9 for ^{16}O–AgBr interactions at 60 AGeV and in figure 10 for ^{32}S–AgBr interactions. The errors shown in the figures are purely statistical. It is seen from the figures that the values of scaled variance increase initially with the increase of rapidity window size. For larger values of $\Delta\eta$, the scaled variance becomes almost constant for all the interactions. In the same figures we have plotted the scaled variance against the rapidity width for the simulated data sets also of all the interactions. The values of scaled variance for the simulated events go on increasing as the rapidity width increases. No saturation effect is observed in the case of simulated events. The experimental results have also been compared with those obtained from analysing events generated by the computer code FRITIOF based on the Lund Monte Carlo model [22,23] for high-energy nucleus–nucleus interaction in ^{16}O–AgBr interactions at 60 AGeV and ^{32}S–AgBr interactions at 200 AGeV. The model assumes that as two nucleons collide with each other, particle production takes place through the creation of longitudinally excited strings between the constituents of the same nucleon. The strings subsequently fragment, and new hadrons originate. A nucleus–nucleus collision is considered to be a combination of multiple collisions between the nucleons belonging to one nucleus with those of the other. A large sample of events has been generated using the code for both the interactions, where the proportional abundance of different categories of target nuclei

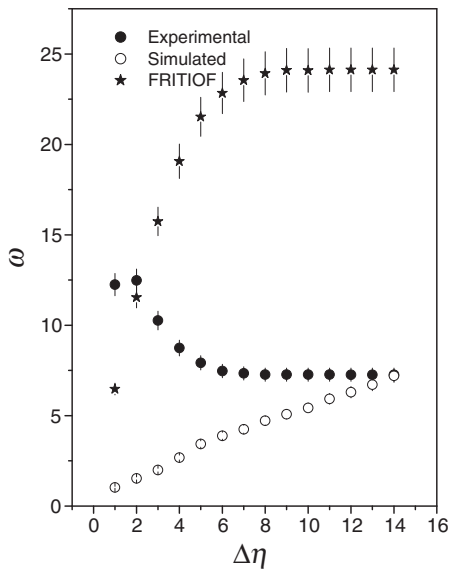

Figure 9. The variation of scaled variance with rapidity window for ^{16}O–AgBr interactions at 60 AGeV for the experimental, simulated and the FRITIOF events for $\Delta\eta = \eta_c - 0.5 \leq \eta_c \leq \eta_c + 0.5$.

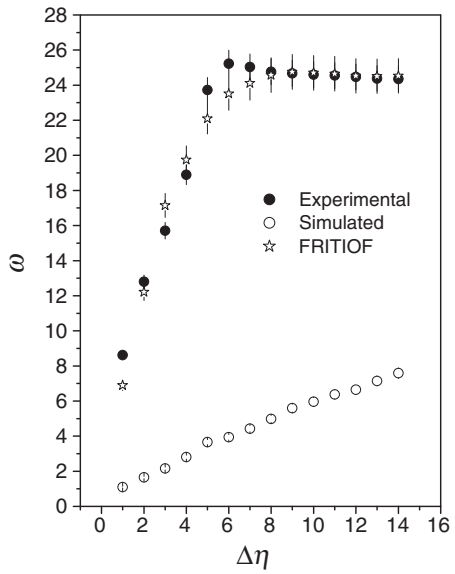

Figure 10. The variation of scaled variance with rapidity window for ^{32}S–AgBr interactions at 200 AGeV for the experimental, simulated and the FRITIOF events when rapidity interval is varied in steps of 1 centring about the central rapidity.

Table 4. The values of scaled variance in different interactions and in different window sizes for the FRITIOF model in ^{16}O–AgBr interactions at 60 AGeV and ^{32}S–AgBr interactions at 200 AGeV when rapidity interval is varied in steps of 1 centring about the central rapidity.

Window size $\Delta\eta$	^{16}O–AgBr interactions at 60 AGeV (FRITIOF)	^{32}S–AgBr interactions at 200 AGeV (FRITIOF)
1	6.47 ± 0.012	6.9 ± 0.013
2	11.54 ± 0.014	12.21 ± 0.017
3	15.74 ± 0.017	17.15 ± 0.018
4	19.07 ± 0.018	19.75 ± 0.020
5	21.53 ± 0.019	22.10 ± 0.022
6	22.84 ± 0.022	23.51 ± 0.023
7	23.55 ± 0.024	24.11 ± 0.026
8	23.93 ± 0.025	24.57 ± 0.032
9	24.10 ± 0.026	24.75 ± 0.033
10	24.09 ± 0.038	24.70 ± 0.037
11	24.12 ± 0.041	24.65 ± 0.040
12	24.12 ± 0.043	24.53 ± 0.041
13	24.12 ± 0.045	24.51 ± 0.044
14	24.12 ± 0.047	24.53 ± 0.045

present in the emulsion material has been taken into account. The scaled variances calculated for ^{16}O–AgBr interactions at 60 AGeV and ^{32}S–AgBr interactions at 200 AGeV are shown in table 4. The variation of scaled variance with the rapidity window size in ^{16}O–AgBr interactions at 60 AGeV and ^{32}S–AgBr interactions are also shown in figures 9 and 10 respectively along with the experimental and simulated values of scaled variance. From figure 9, it is quite clear that the FRITIOF data for ^{16}O–AgBr interactions

Table 5. The values of scaled variance in different interactions and in different window sizes when rapidity interval is varied in steps of 1.6 centring about the central rapidity.

Window size $\Delta\eta$	^{16}O–AgBr interactions at 2.1 AGeV	^{24}Mg–AgBr interactions at 4.5 AGeV	^{12}C–AgBr interactions at 4.5 AGeV	^{16}O–AgBr interactions at 60 AGeV	^{32}S–AgBr interactions at 200 AGeV
1.6	2.93 ± 0.002	2.85 ± 0.002	3.14 ± 0.004	12.89 ± 0.010	10.77 ± 0.010
3.2	2.91 ± 0.006	4.47 ± 0.006	3.32 ± 0.008	10.00 ± 0.012	15.07 ± 0.011
4.8	2.71 ± 0.008	4.41 ± 0.008	3.15 ± 0.010	8.08 ± 0.015	20.28 ± 0.015
6.4	2.40 ± 0.010	4.27 ± 0.012	2.92 ± 0.014	7.36 ± 0.018	22.42 ± 0.017
8.0	2.26 ± 0.013	4.14 ± 0.013	2.78 ± 0.019	7.26 ± 0.019	22.12 ± 0.018
9.6	2.19 ± 0.015	4.02 ± 0.018	2.68 ± 0.019	7.26 ± 0.019	21.95 ± 0.018
11.2	2.19 ± 0.019	3.96 ± 0.019	2.68 ± 0.019	7.26 ± 0.019	21.87 ± 0.021
12.8	2.2 ± 0.019	3.97 ± 0.025	2.68 ± 0.019	7.26 ± 0.019	21.74 ± 0.023
14.4	2.2 ± 0.022	4.00 ± 0.027	2.68 ± 0.019	7.26 ± 0.019	21.68 ± 0.024

Table 6. The values of scaled variance in different interactions and in different window sizes when rapidity interval is varied in steps of 1.6 centring about the central rapidity for the simulated events.

Window size $\Delta\eta$	^{16}O–AgBr interactions at 2.1 AGeV (simulated events)	^{24}Mg–AgBr interactions at 4.5 AGeV (simulated events)	^{12}C–AgBr interactions at 4.5 AGeV (simulated events)	^{16}O–AgBr interactions at 60 AGeV (simulated events)	^{32}S–AgBr interactions at 200 AGeV (simulated events)
1.6	0.64 ± 0.002	0.654 ± 0.001	0.45 ± 0.002	1.33 ± 0.001	1.48 ± 0.001
3.2	0.904 ± 0.002	1.09 ± 0.002	0.859 ± 0.006	2.18 ± 0.005	2.36 ± 0.002
4.8	1.033 ± 0.005	1.4 ± 0.007	1.23 ± 0.009	3.26 ± 0.007	3.52 ± 0.007
6.4	1.231 ± 0.007	1.68 ± 0.008	1.45 ± 0.010	4.13 ± 0.008	4.23 ± 0.010
8.0	1.295 ± 0.009	1.98 ± 0.009	1.55 ± 0.011	4.72 ± 0.009	4.98 ± 0.012
9.6	1.47 ± 0.010	2.28 ± 0.010	1.75 ± 0.014	5.26 ± 0.009	5.83 ± 0.013
11.2	1.54 ± 0.012	2.55 ± 0.011	1.97 ± 0.016	5.98 ± 0.010	6.40 ± 0.015
12.8	1.85 ± 0.013	3.07 ± 0.015	1.99 ± 0.018	6.17 ± 0.012	7.08 ± 0.016
14.4	2.00 ± 0.015	3.17 ± 0.016	2.09 ± 0.019	6.39 ± 0.013	7.69 ± 0.016

at 60 AGeV do not support the experimental data. However, for ^{32}S–AgBr interactions the experimental findings are well supported by the FRITIOF model. To see the effect of binning on the occurrence the multiplicity fluctuations, the whole analysis was repeated for experimental, simulated and the FRITIOF data again. The interval size was taken as $\Delta\eta = \eta_c - 0.8 \leq \eta_c \leq \eta_c + 0.8$. The value of $\Delta\eta$ was increased in steps of 1.6 till it reached 14.4. The scaled variance was calculated in each of this rapidity interval for all the interactions. The values of the scaled variance for this interval size is given in table 5 for the

Table 7. The values of scaled variance in different interactions and in different window sizes for the FRITIOF model in ^{16}O–AgBr interactions at 60 AGeV and ^{32}S–AgBr interactions at 200 AGeV when rapidity interval is varied in steps of 1.6 centring about the central rapidity.

Window size $\Delta\eta$	^{16}O–AgBr interactions at 60 AGeV (FRITIOF)	^{32}S–AgBr interactions at 200 AGeV (FRITIOF)
1.6	10.17 ± 0.011	9.607 ± 0.012
3.2	17.16 ± 0.015	18.02 ± 0.015
4.8	22.22 ± 0.021	21.42 ± 0.020
6.4	24.42 ± 0.022	23.83 ± 0.022
8.0	25.29 ± 0.025	24.57 ± 0.023
9.6	25.47 ± 0.027	24.75 ± 0.026
11.2	25.49 ± 0.029	24.63 ± 0.028
12.8	25.48 ± 0.030	24.62 ± 0.032
14.4	25.48 ± 0.030	24.58 ± 0.034

experimental data set, in table 6 for the simulated data set and in table 7 for the FRITIOF data sets. Comparing the values of scaled variance of table 1 with table 5, table 3 with table 6 and table 4 with table 7 it is clear that the values of ω do not differ significantly for the experimental, simulated and the FRITIOF data set for the present case from the values obtained when the analysis was performed by varying the interval size in steps of 1. We have also plotted scaled variance against rapidity window size for experimental, simulated and FRITIOF data set in figure 11 for ^{16}O–AgBr interactions at 2.1 AGeV, in figure 12 for ^{24}Mg–AgBr interactions, in figure 13 for ^{12}C–AgBr interactions, in figure 14 for ^{16}O–AgBr interactions at 60 AGeV and in figure 15 for ^{32}S–AgBr interactions. The nature of variations of scaled variance with rapidity window sizes are almost the same as obtained in the previous binning condition. As before, the experimental data cannot be explained by the FRITIOF model for ^{16}O–AgBr interactions at 60 AGeV. We have also noted the region of maximum fluctuations when the interval size is varied in steps of 1.6 for all the interactions and tabulated in table 8. From table 8 it can be seen that the maximum fluctuations for ^{16}O–AgBr interactions at 2.1 AGeV has occurred in the rapidity interval $0.2 \leq \eta_c \leq 2.0$. For ^{12}C–AgBr and ^{24}Mg–AgBr interactions, the maximum values of scaled variance have occurred in the rapidity interval $0.0 \leq \eta_c \leq 3.2$ and $0.6 \leq \eta_c \leq 3.8$, respectively. For ^{16}O–AgBr interactions at 60 AGeV and ^{32}S–AgBr interactions, the dynamical fluctuations are found to be maximum in the rapidity range $1.2 \leq \eta_c \leq 2.8$ and $1.5 \leq \eta_c \leq 7.9$ respectively. If we compare tables 2 and 8 it can be said that at higher energies the rapidity range of maximum fluctuations remains almost the same as the binning condition is changed.

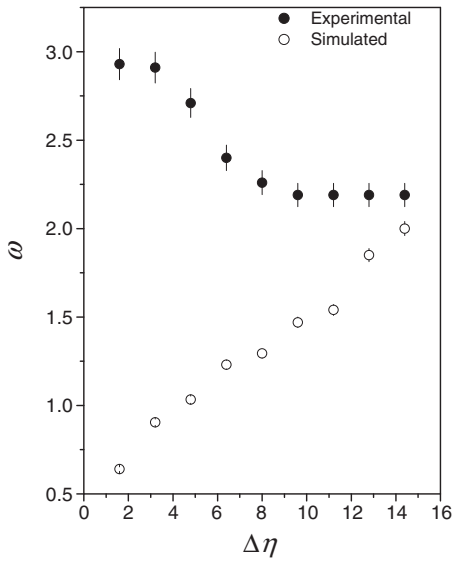

Figure 11. The variation of scaled variance with rapidity window for ^{16}O–AgBr interactions at 2.1 AGeV for the experimental and the simulated events when rapidity interval is varied in steps of 1.6 centring about the central rapidity.

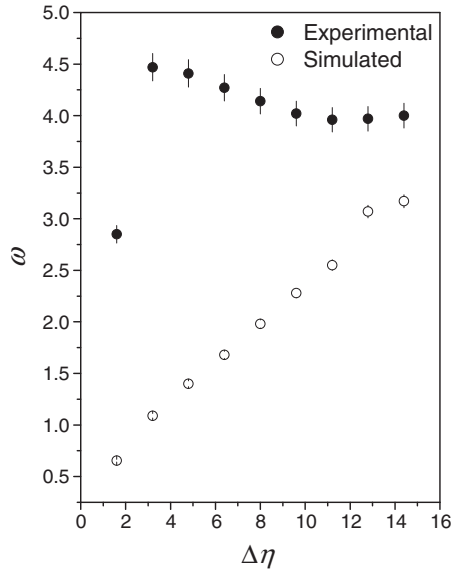

Figure 12. The variation of scaled variance with rapidity window for ^{24}Mg–AgBr interactions at 4.5 AGeV for the experimental and the simulated events when rapidity interval is varied in steps of 1.6 centring about the central rapidity.

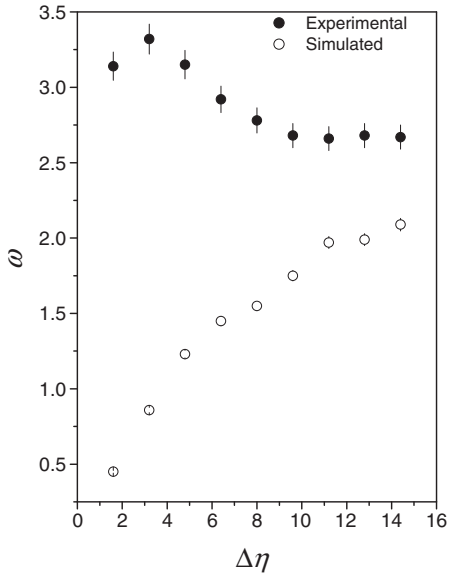

Figure 13. The variation of scaled variance with rapidity window for ^{12}C–AgBr interactions at 4.5 AGeV for the experimental and the simulated events when rapidity interval is varied in steps of 1.6 centring about the central rapidity.

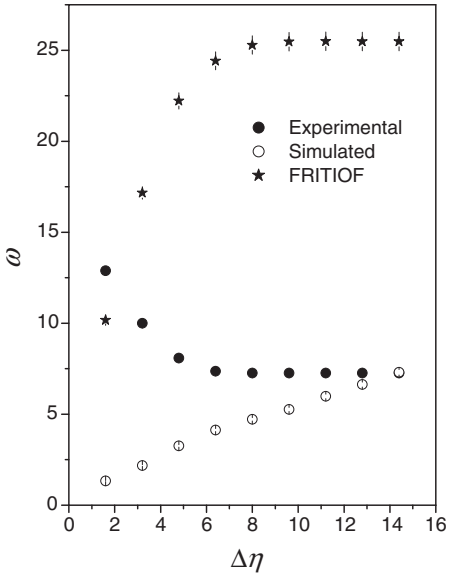

Figure 14. The variation of scaled variance with rapidity window for ^{16}O–AgBr interactions at 60 AGeV for the experimental, simulated and the FRITIOF events when rapidity interval is varied in steps of 1.6 centring about the central rapidity.

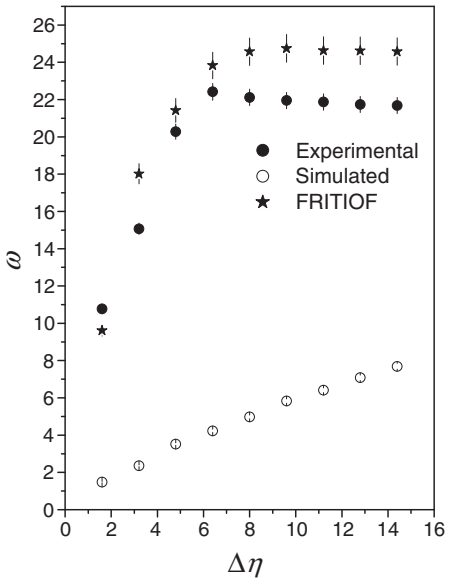

Figure 15. The variation of scaled variance with rapidity window for ^{32}S–AgBr interactions at 200 AGeV for the experimental, simulated and the FRITIOF events when rapidity interval is varied in steps of 1.6 centring about the central rapidity.

Table 8. The maximum value of scaled variance for different interactions and at different rapidity width where maximum fluctuations occurred when rapidity interval is varied in steps of 1.6 centring about the central rapidity.

Interactions	Energy (AGeV)	$\Delta\eta$ Range	$\omega_{\max}$
^{16}O–AgBr	2.1	$0.2 \leq \eta_c \leq 2.0$	2.93 ± 0.002
^{12}C–AgBr	4.5	$0.0 \leq \eta_c \leq 3.2$	3.32 ± 0.008
^{24}Mg–AgBr	4.5	$0.6 \leq \eta_c \leq 3.8$	4.47 ± 0.006
^{16}O–AgBr	60	$1.2 \leq \eta_c \leq 2.8$	12.89 ± 0.012
^{32}S–AgBr	200	$1.5 \leq \eta_c \leq 7.9$	22.42 ± 0.017

From table 8 it can be noted that the value of $\omega_{\max}$ is minimum for ^{16}O–AgBr interactions at 2.1 AGeV. The value of $\omega_{\max}$ for ^{24}Mg–AgBr interactions are higher than that for ^{12}C–AgBr interactions. These are consistent with our earlier findings. Comparing tables 2 and 8 it may be said that the values $\omega_{\max}$, when the interval is varied in steps of 1.6, are little less than that when the interval is varied in steps of 1.

To find out the nature of correlation among the produced pions from a few GeV to a few hundred GeV, in terms of the scaled variance ω, we see from tables 1 and 5 that for all the interactions and all the rapidity window sizes, the values of ω are well above 1 for the experimental data sets. This observation implies that the multiplicity distribution deviates from the Poissonian distribution everywhere. The deviation from Poisson distribution shows the presence of correlated production of pions. Maximum values of scaled variance indicate maximum correlation and their region of maximum fluctuations depicts the region of maximum correlation. Also from the variation of scaled variance with the rapidity window sizes, for the experimental data sets, it is noticeable that the correlations among the produced pions increase with the increase of rapidity width and later saturates at larger rapidity window. This presence of correlation among the produced pions indicates the occurrence of non-statistical fluctuation during the multiparticle production process.

References

[1] H Heiselberg, *Phys. Rep.* **351**, 161 (2001)
[2] C Alt *et al*, *Phys. Rev*. **C78**, 034914 (2008)
[3] V V Begun, M Gaździcki, M I Gorenstein and O S Zozulya, *Phys. Rev*. **C70**, 034901 (2004)
[4] V V Begun, M I Gorenstein, A P Kostyuk and O S Zozulya, *Phys. Rev*. **C71**, 054904 (2005)
[5] V V Begun *et al*, *Phys. Rev*. **C76**, 024902 (2007)
[6] B Lungwitz and M Bleicher, *Phys. Rev*. **C76**, 044904 (2007)
[7] V P Konchakovski *et al*, arXiv:0712.2044[nucl. Th] 11pages
[8] NA49 Collaboration: H Appelshäuser *et al*, *Phys. Lett.* **B459**, 679 (1999)
[9] NA49 Collaboration: G Roland *et al*, *Nucl. Phys.* **A638**, 91c (1998)
[10] M Stephanov, K Rajagopal and E Shuryak, *Phys. Rev*. *Lett.* **81**, 4816 (1998)
[11] G Baym, G Friedman and I Sarcevic, *Phys. Lett.* **B219**, 205 (1989)
[12] R Albrecht *et al*, *Z. Phys.* **C45**, 31 (1989)
[13] D Ghosh, P Ghosh and A Ghosh, *Phys. Rev*. **C49**, R1747 (1994)

[14] D Ghosh, J Roy and R Sengupta, *Nucl. Phys.* **A468**, 719 (1987)
[15] D Ghosh, A Mukhopadhyay, A Ghosh and J Roy, *Mod. Phys. Lett.* **A4**, 1197 (1989)
[16] K Sengupta, P L Jain, G Singh and S N Kim, *Phys. Lett.* **B236**, 219 (1989)
[17] C F Powell, P H Fowler and D H Perkins, *The study of the elementary particles by photographic method* (Pergamon Press, Oxford, UK, 1959) pp. 450–464
[18] D Ghosh, B Biswas, A Deb and J Roy, *Phys. Rev*. **C56**, 2879 (1997)
[19] D Ghosh, P Ghosh, A Ghosh and J Roy, *J. Phys.* **G20**, 1077 (1994)
[20] D Ghosh *et al*, *Phys. Rev*. **C59**, 2286 (1999)
[21] D Ghosh *et al*, *Phys. Rev*. **C52**, 2092 (1995)
[22] B Andersson, G Gustafson and B Nilsson-Almqvist, *Nucl. Phys.* **B281**, 289 (1987)
[23] B Nilsson-Almquist and E Stenlund, *Comput. Phys. Commun.* **43**, 387 (1987)